International Journal of Environmental Science and Technology (2026) 23:157
https://doi.org/10.1007/s13762-025-06808-4

ORIGINAL PAPER

Fabrication of AgI/ZnO photocatalyst for mechanistic study and photodegradation of tetracycline

A. N. Muhamad Hissam[1] · S. I. Sinar Mashuri[1,2] · N. F. Chayed[1,2] · N. H. Rozali Annuar[3] · N. Asikin-Mijan[4] · S. F. Ibrahim[5] · N. H. Othman[6] · G. AbdulKareem-Alsultan[7,8] · Y. H. Tan[9] · U. Rashid[10] · Y. H. Taufiq-Yap[7,8] · M. L. Ibrahim[1,2]

Received: 9 June 2024 / Revised: 26 September 2024 / Accepted: 29 October 2025

Abstract
Tetracycline is an antibiotic known to inhibit the growth of microorganisms in soil and water. Often, pharmaceutical companies release unwanted and expired antibiotics, leading to water pollution. This study involved the synthesis of AgI combined with ZnO to form heterostructures by a wet impregnation method to degrade tetracycline molecules. The primary objective is to explore the mechanistic pathways of tetracycline degradation under visible light irradiation. The combination of AgI and ZnO is chosen due to their enhanced photocatalytic properties when coupled, as ZnO provides a stable, wide-bandgap semiconductor, while AgI improves visible light absorption, extending the efficiency of the catalyst. Catalyst characterization by Field Emission Scanning Electron Microscopy with Energy Dispersive X-Ray Spectroscopy analysis confirmed the presence of AgI and ZnO phases, while X-ray Diffraction showed distinct crystalline structures of both. Surface area analysis indicated a controlled pore volume of 31.78 nm and a high surface area of 27.29 m^2/g for the AgI/ZnO composites. The Tauc plot demonstrated that AgI doping reduced the ZnO optical energy bandgap from 3.39 to 2.83 eV. The AgI/ZnO catalyst achieved up to 89.38% degradation of tetracycline at 10 mg/L concentration using 0.01 g of AgI/ZnO, under a 150-W metal halide lamp at pH 9 in 90 min. Scavenger tests identified superoxide radicals and electrons as the primary species facilitating tetracycline photodegradation. The AgI/ZnO photocatalysts showed remarkable reusability, maintaining efficiency over five cycles. Therefore, AgI/ZnO holds great potential as an effective photocatalyst for breaking down organic pollutants like tetracycline using visible light energy.

Keywords AgI/ZnO · Degradation · Organic pollutant degradation · Photocatalysis · Tetracycline · Wastewater

Introduction

Antibiotic pollution is emerging due to the widespread use of antibiotics in human healthcare, agriculture, and the pharmaceutical and medical industries. One antibiotic significantly contributing to water pollution and environmental concerns is tetracycline (TC) (Fiaz et al., 2021; Amangelsin et al. 2023; Gokul et al. 2023). TC residues possess antimicrobial properties that inhibit the growth of microorganisms in both soil and water (Zhan et al. 2021). Based on previous study by Amangelsin et al. (2023), they found that the TC concentration in the waterbodies in range 0.25–30 mg/L. Therefore, it is crucial to decompose TC into harmless compounds to mitigate its environmental impact. However, due to its chemical stability and antibacterial characteristics, breaking down TC is extremely challenging (Semeraro et al. 2020; Doosti et al. 2022; Jia et al. 2022). The degradation of organic contaminants generally occurs through chemical, physical, or biological methods. Among these, chemical techniques offer precise control over conditions and can increase the degradation rate. Chemical methods, including electrochemical pathways, sonolysis, photocatalysis, ozonation, photo-Fenton, and Fenton's reaction, are key components of advanced oxidation technologies (Boxi 2024; Drwal et al. 2022). According to previous reports (Nguyen et al. 2020; Amiruddin et al. 2021), photocatalytic approaches effectively remove pathogens, viruses, detergents, pesticides, and various conventional and emerging organic pollutants. Thus, employing photocatalysis for degrading organic pollutants is promising, as advanced oxidation processes

Editorial responsibility: Samareh Mirkia.

Extended author information available on the last page of the article

Published online: 15 December 2025

(AOPs) can lead to complete mineralization during degradation while enhancing cost-effectiveness (Pavel et al. 2023).

The photocatalytic degradation process starts with the photogeneration of electron–hole (e^-/h^+) pairs (Ibrahim et al. 2023). This process generates hydroxyl radicals (·OH) when hole (h^+) oxidizes surface-absorbed water molecules (H_2O) or hydroxide ions (OH^-). Additionally, photoexcited electron (e^-) reduce oxygen molecules (O_2) to form hydroperoxyl or superoxide radicals ($\cdot O_2^-$) (Ahmed and Mohamed 2023; Li et al. 2023). Reactive oxygen species (ROS) (e.g., ·OH, $\cdot O_2^-$) and free h^+ interact with surface-absorbed molecules, such as organic and inorganic compounds, during the photocatalytic process following series reactions Eqs. 1–5, transforming pollutants into harmless by-products (Ibrahim et al. 2024).

$$\text{Semiconductor} + hv \rightarrow h^+ + e^- \quad (1)$$

$$e^- + h^+ \rightarrow \text{energy} \quad (2)$$

$$h^+ + H_2O \rightarrow \cdot OH + H^+ \quad (3)$$

$$e^- + O_2 \rightarrow \cdot O_2^- \quad (4)$$

$$\text{ROS} + \text{pollutant} \rightarrow \text{degradation product} \quad (5)$$

Zinc oxide (ZnO) is a popular photocatalyst due to its unique electrical properties, low production cost, and availability (Mao et al. 2022; Güell et al. 2023). However, its wide bandgap (3.2 eV) restricts its absorption to ultraviolet (UV) light, which constitutes only a small fraction (~4%) of the solar spectrum (Kaus et al., 2022; Tegenaw et al. 2023; Shohaimi et al. 2024). Additionally, the recombination of excited e^- and h^+ under UV light significantly reduces photocatalytic efficiency. To enhance ZnO's photocatalytic performance, strategies such as element doping, and semiconductor coupling have been employed (Ramírez et al. 2021; Luu et al. 2024). These methods include doping ZnO with narrow-gap semiconductors to facilitate the separation of e^-/h^+ pairs and shift the absorption band to the visible light region (Mashuri et al. 2020; Moiz et al. 2021). This indicates that doping ZnO with narrow-gap semiconductors can effectively tailor its optical bandgap, increase degradation efficiency, enhance ·OH generation, and decrease recombination rates (Talreja et al. 2021). Therefore, this approach is highly effective for neutralizing antibiotic pollutants in wastewater treatment processes.

AgI is a semiconductor with a narrow bandgap around 2.8 eV (Zhou et al. 2020). Thus, it could be easily absorbing photons from the visible light (Liu et al. 2021). As the visible light absorber, AgI shows high potential as film-based photography (Sayyed et al. 2022), solar cells (Arjmand et al. 2022), colorimetric detector (Cao et al. 2024) and conductive coating (Tang et al. 2024). Due to its photosensitive properties, AgI shows high potential to improve the ZnO-based photocatalyst as it has strong capacity for absorption of visible light and produce electron and hole pair as required to degrade the organic pollutant such as TC (Zarezadeh et al. 2020).

The coupling of ZnO with AgCl, AgBr and various ternary nanocomposites (such as ZnO/AgI/Fe_3O_4 and ZnO/AgI/Ag_2CO_3) has garnered significant interest due to the narrow bandgap of semiconductors like AgX (X = Cl, Br, I), which are compatible with ZnO (Taghizadeh et al. 2020; Liu et al. 2021). In this study, silver iodide (AgI) was introduced into the ZnO semiconductor photocatalyst because it has a narrow bandgap and high photosensitivity, enabling more efficient solar energy utilization. Additionally, AgI incorporation increases the surface area of the composite, providing more active sites for photocatalytic reactions. The incorporation of AgI with ZnO is expected to produce a synergistic heterostructure, extending the absorption range of ZnO and enhancing its photocatalytic efficiency in TC degradation. The photo-deposition of AgI onto ZnO contributed to a uniform distribution of the AgI layer and formed a tight interaction with ZnO, preventing agglomeration and facilitating effective charge transfer between the two components (Ding et al. 2020). Additionally, AgI acts as a photosensitizer, transferring photogenerated electrons to ZnO, resulting in more electron-hole pairs available for TC degradation. The stable interaction between AgI and ZnO also minimizes the leaching of AgI into the environment, making the composite more environmentally friendly (Ghattavi and Nezamzadeh-Ejhieh 2019; Rajput et al. 2022; Pham et al. 2023). Furthermore, the photo-deposition method is scalable, simple, and cost-effective, making it practical for widespread applications (Kadem et al. 2023).

This work focuses on preparation and characterization of AgI/ZnO photocatalysts by wet impregnation technique, and to evaluate their efficiency in degrading TC molecules in water under visible light irradiation assisted with metal halide lamp. The study aims to determine the effectiveness of the AgI/ZnO photocatalyst in removing TC, investigate the reactive species involved in the degradation process, assess the photocatalyst's reusability over multiple cycles, and explore the mechanistic pathways of TC degradation under visible light, with AgI enhancing visible light absorption and ZnO providing a stable, wide-bandgap semiconductor for improved photocatalytic efficiency.

The study was held at Faculty of Applied Science, Universiti Teknologi MARA (UiTM) Shah Alam Selangor, since January 2022.

Materials and methods

Materials

The TC compound ($C_{22}H_{24}N_2O_8$, purity ≥ 99%) was purchased from Chemiz (Malaysia). Silver nitrate ($AgNO_3$, purity ≥ 99.5%), potassium iodide (KI, purity ≥ 98%), and ZnO, purity ≥ 99%) were purchased from SYSTERM (ChemPur). Methanol (CH_3OH) and sodium hydroxide (NaOH) were purchased from Chemiz (Malaysia), while hydrochloric acid (HCl) was bought from Fisher Scientific (M) SDN BHD. 1,4-benzoquinone (p-BQ) ($C_6H_4O_2$, purity ≥ 98%) and Ethylenediaminetetraacetic acid (EDTA) ($C_{10}H_{16}N_2O_8$, purity ≥ 98.5%) were purchased from Sigma-Aldrich. Isopropyl alcohol (IPA) (C_3H_8O, purity 99%) was purchased from QReC. All the materials were utilized as received without any additional treatment or purification.

Synthesis of AgI doped-ZnO photocatalyst

A simple three-step procedure was used to prepare the AgI/ZnO composites. First, to ensure even dispersion of the ZnO particles, 20 mL of a 0.1 M $AgNO_3$ solution was added to 0.81 g of ZnO in a 100 mL beaker, and the mixture was swirled for 10 min. Then, after stirring for 30 min, 20 mL of a 0.1 M KI solution was gradually added to complete the conversion of Ag^+ and I^- to AgI. After an hour of stirring, the resulting light-yellow liquid was suction filtered to collect the synthetic composites, which were then dried at 60 °C for three hours (Ding et al. 2021).

Characterization of AgI/ZnO photocatalyst

The JEOL JSM-7600F field emission scanning electron microscope (FESEM) provided quantitative elemental analysis at magnifications ranging from 10× to 300,000×. Particle size distribution was calculated using ImageJ software. The JEOL JEM-2011F high-resolution transmission electron microscope (HRTEM) was used with an accelerating voltage of 200 kV. The photocatalyst's crystallinity was determined using the Debye–Scherrer formula from the X-Ray Diffraction (XRD) diffractogram, with Cu Kα radiation (40 kV, 40 mA). The Brunauer–Emmett–Teller (BET) method characterized the surface area, pore size, pore volume, and mesoporous materials, with adsorption and desorption isotherms measured using a Belsorp mini II. The optical characteristics (transmittance, reflectance, and absorbance) of liquids and solids were determined using a Perkin Elmer Lambda 950 UV–Vis Near-Infrared (UV/Vis–NIR) Spectrometer, which covers a wavelength range from 175 to 3300 nm, extending into the near-infrared (NIR) region.

Adsorption and photocatalytic evaluation of AgI/ZnO photocatalyst

Using a 250-W metal halide lamp with a cut-off filter of 420 nm, the photocatalytic activity of the AgI/ZnO photocatalyst for the degradation of TC was assessed. About 0.1 g of AgI/ZnO photocatalyst was dissolved in a 100 ml solution of distilled water containing 10 ppm of TC. Thus, about 10 mg/L concentration was chosen as it reflects typical levels found in industrial wastewater and polluted rivers, making the experiment environmentally relevant while allowing for benchmarking against similar studies to ensure comparability of results (Liu et al. 2024; Ou et al. 2024; You and Jung 2024). The resultant suspension solutions were constantly magnetically agitated to stir the solution well. Then, the solution was maintained at ambient temperature (≤ 30 °C) by installed the cooling system to adhere to the temperature conditions and prevent overheating as to ensure the consistency of the experiment to mimic the real environment and subjected to visible light irradiation for 90 min. About 5 ml of the visible light-irradiated solutions were taken at 30 min intervals and centrifuged for 10 min to determine the amount of TC degradation before being evaluated using UV–visible spectroscopy. Equation 6, as presented below, was utilized to determine the removal efficiency of TC by the photocatalyst (Semeraro et al. 2020).

$$\text{Removal Efficiency} = \left(\left(C_o - C_t\right)/C_o\right) \times 100\% \quad (6)$$

where C_o and C_t are the TC concentrations (mg/L) at the initial stage and degradation times, respectively.

For adsorption test, about 0.01 g of AgI/ZnO was added to 100 mL of 10 mg/L TC solution. The reaction was recorded as well as how long it took to get a constant percentage. The constant percentage indicates the achievement of maximal adsorption. The photolysis test was done by 100 mL of 10 mg/L TC solution exposed to 150-W of metal halide source for about 90 min. The TC solution was observed in 15 min intervals. Lastly, the percentage degradation was determined.

For degradation of TC molecules, the photocatalytic activity was repeated to all six parameters which are the initial concentration of TC solution (6, 8, 10, 12 and 14 ppm), photocatalyst dosage (0.01, 0.02, 0.03 and 0.04 g), the light intensity (150-W metal halide lamp, 250-W metal halide lamp, and LED), the pH of the TC (pH 3, 7 and 9) the recyclability of the catalyst, and the Scavenger test (p-BQ, IPA, $AgNO_3$, and EDTA (Tofanello et al. 2021; Azqandi et al. 2023).

Scavenger test for generated actives sites

A 100 mL solution containing 10 mg/L of TC at pH 9 was mixed with roughly 0.3 mL of a 0.05 M $AgNO_3$ solution, serving as a scavenger reagent, along with 0.01 g of AgI/ZnO to identify the active e^- species. The reaction mixture was then exposed to a 150-W metal halide lamp for a duration of ninety minutes. Subsequent to the reaction, a 3 mL aliquot of the TC solution was collected and analyzed using a Thermo Scientific Genesys 30 UV–Visible spectrophotometer to determine the concentration. This experimental procedure was repeated to investigate the presence of other active species, namely h^+, ·OH, and $\cdot O_2^-$, utilizing different scavenger reagents including 1.0 M EDTA, IPA, and p-BQ.

Recyclability test

To examine the stability of the AgI/ZnO photocatalyst, a recyclability test was performed. The spent catalyst was separated from the TC solution using double filter sheets (Whatman, 41, 125 mm, CAT no. 1441-125). Before initiating the next reaction for reusability cycle under same conditions, the spent catalyst was cleaned and dried at 50 °C. Fresh TC solution was prepared for each cycle. At the end of each cycle, approximately 3 mL of solution was collected to measure the degradation of TC.

Results and discussion

Catalyst characterization

The FESEM and HRTEM images are illustrated in Fig. 1. Figure 1a displays the ZnO catalyst exhibiting hexagonal wurtzite and cubic zincblende shapes, while AgI/ZnO composites in Fig. 1b exhibit a flower-like structure. The results were aligned with XRD crystal system where the ZnO and AgI/ZnO reveal a hexagonal wurtzite ZnO structure adorned with cubic AgI nanoparticles. This configuration indicates that AgI was incorporated onto the ZnO catalyst which can enhance the surface area that is crucial in photocatalytic activity (Guo et al. 2022). It can be observed from TEM analysis shown in Fig. 1c.

The results revealed that AgI was distributed evenly and with consistent particle size across the samples, indicating that ZnO maintaining its regular form after modification (Ding et al. 2020). The interplanar crystal spacings of 0.2412 nm for AgI (1 1 1) and 0.337 nm for ZnO (0 0 2) consistent with XRD patterns as shown in Fig. 1d. Reported that an increase in the photodegradation of TC with the increase of loaded content of AgI onto the surface of ZnO. Thus, the extensive surface area of powdered material facilitates a larger reaction area for target molecules, potentially enhancing degradation rates by absorbing more contaminants.

The crystalline nature of AgI/ZnO materials was confirmed through analysis by the Joint Committee on Powder Diffraction Standards (JCPDS), with XRD patterns depicted in Fig. 2a**.** Examination of the XRD pattern for ZnO revealed characteristic peaks at 2θ = 31.78°, 34.42°, 36.26°, 47.54°, 56.60°, 62.86°, 67.94°, and 69.08°, consistent with the hexagonal structure of ZnO according to the International Centre for Diffraction Data (JCPDS 00-005-0664). The XRD pattern illustrates that AgI crystals manifest two distinct morphologies: cubic zinc blende-type (γ-AgI) peaks observed at 2θ = 39.20° and 46.33°, and hexagonal wurtzite-type (β-AgI) peaks at 2θ = 22.35° and 23.71°. Obtaining pure crystals of a single phase is typically challenging; however, the presence of AgI in this study closely aligns with a β-AgI phase, corroborated by JCPDS No. 01-078-0641.

The dispersion of AgI within the ZnO crystal matrix was confirmed by the presence of both AgI and ZnO peaks in the AgI/ZnO composite graph. The distinct separation of ZnO and AgI peaks indicates that the incorporation of AgI did not alter the ZnO crystalline phase in the nanocomposites, with diffraction peaks readily assignable to AgI and ZnO components. The crystallite size (L) of AgI/ZnO was calculated to be 76.22 nm using the Debye–Scherrer equation, as demonstrated in Eq. 7.

$$\text{Crystallite size}(L) = k\lambda/\beta\cos \tag{7}$$

where θ is the diffraction angle, 0.9 is the form factor, K is the wavelength of the CuKα utilized, and β is the whole breadth at half maximum of the diffraction angle taken into consideration.

The isotherm plot displaying the hysteresis for mesoporous AgI/ZnO is presented in Fig. 2b. The graph indicates that AgI/ZnO owing to type IV adsorption which the excellent properties can increase the photocatalytic activity in both adsorption and desorption (Chayed et al. 2023). The type of pores of the photocatalyst is mesoporous, as it ranges between 2 and 50 nm. From Table 1, the surface area of AgI/ZnO is larger compared to ZnO. The surface area of AgI/ZnO using BET method exhibits a higher value of 27.969 $m^2\ g^{-1}$ demonstrating superior porosity and surface properties. These characteristics influence the adsorption of the contaminants. The increase surface of photocatalyst lead to greater number of actives sites, thereby enhancing the photodegradation of organic substrates (Khalit et al. 2020; Ding et al. 2020).

The UV–VIS-NIR analysis was conducted to examine the reflectance edge of the AgI/ZnO photocatalyst, revealing a range of 410–470 nm, as illustrated in Fig. 3a). This spectral range signifies the capability of AgI/ZnO to be activated by visible light. The bandgap energies of ZnO and AgI/ZnO

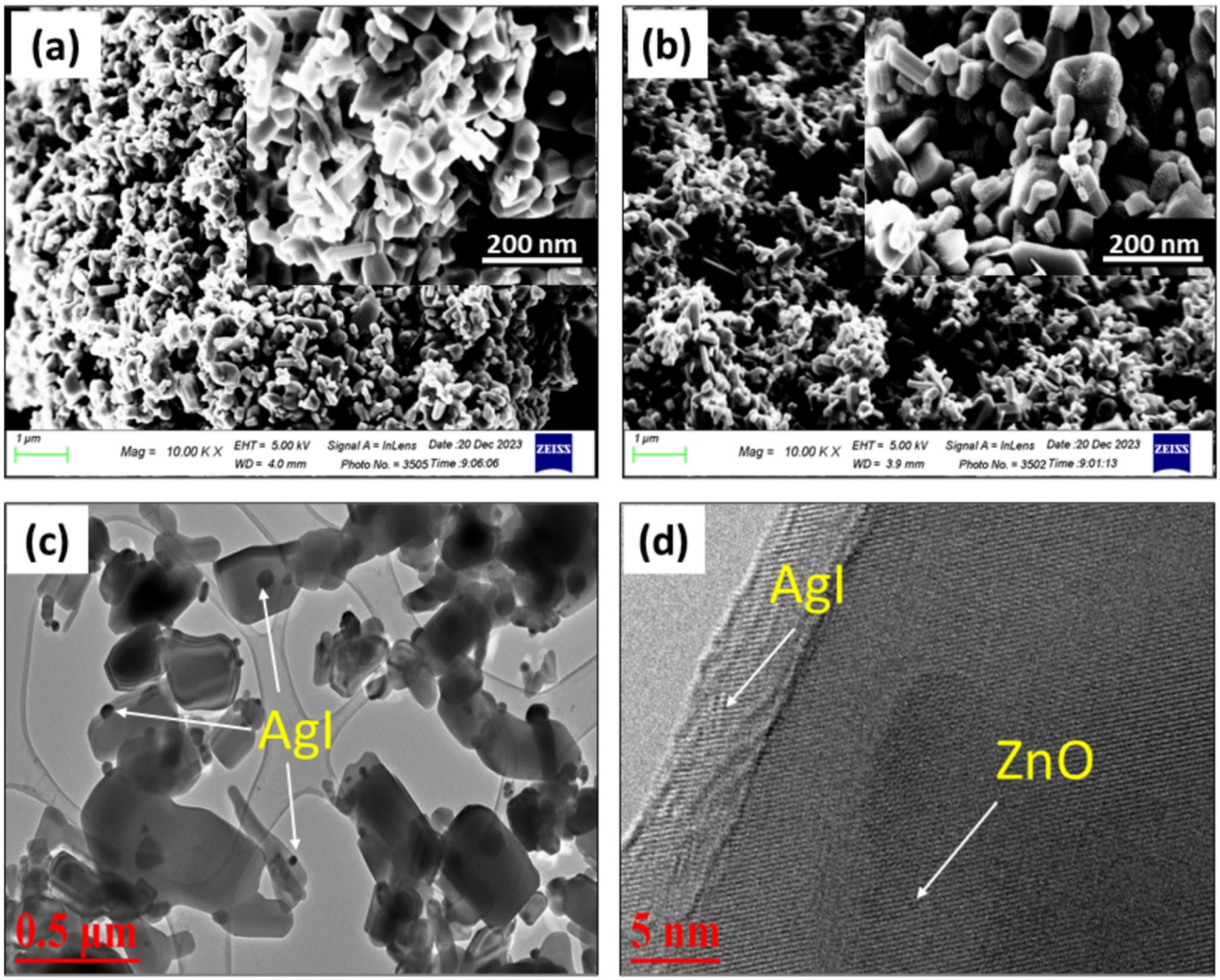

Fig. 1 FESEM images of **a** ZnO at 10.00 K X **b** AgI/ZnO at 10.00 K X, **c** HRTEM images of AgI/ZnO at 0.5 μm and **d** Interplanar d-spacing

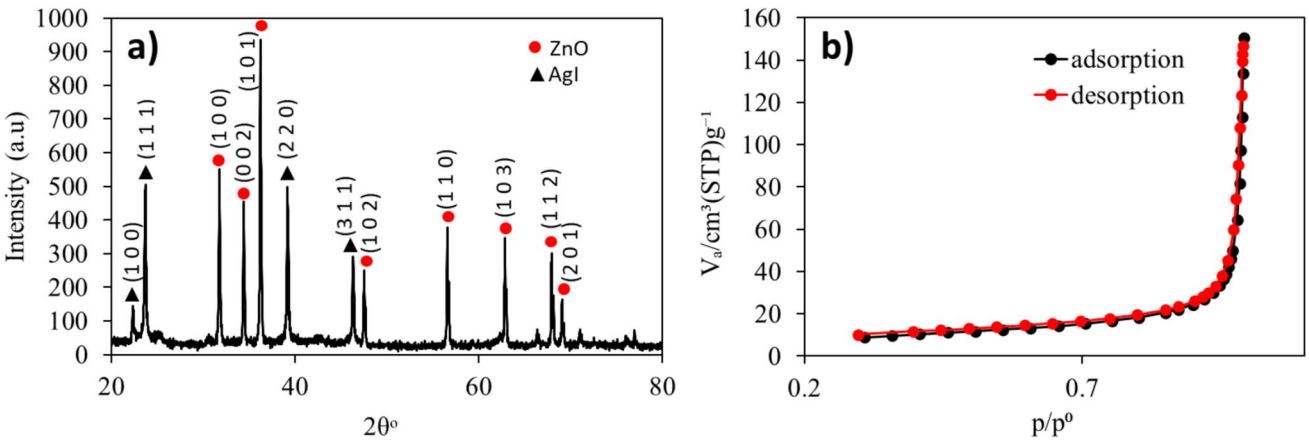

Fig. 2 **a** XRD diffractogram of AgI/ZnO and **b** N_2-adsorption desorption of AgI/ZnO

Table 1 Surface characteristics analysis of AgI/ZnO photocatalyst

Samples	Total pore volume ($cm^3\ g^{-1}$)	Mean pore volume (nm)	Surface area ($m^2\ g^{-1}$)	Types of pores	Ref
ZnO	0.1490	43.558	13.713	Mesoporous	(Mashuri et al. 2023)
ZnO	87.43	0.3536	16.18	Mesoporous	
ZnO	5.18	0.0162	12.54	Mesoporous	(Zarezadeh et al. 2020)
AgI/ZnO	33.55	–	3.41	Mesoporous	(Wu et al. 2021)
AgI/ZnO	0.2166	31.748	27.296	Mesoporous	Present study

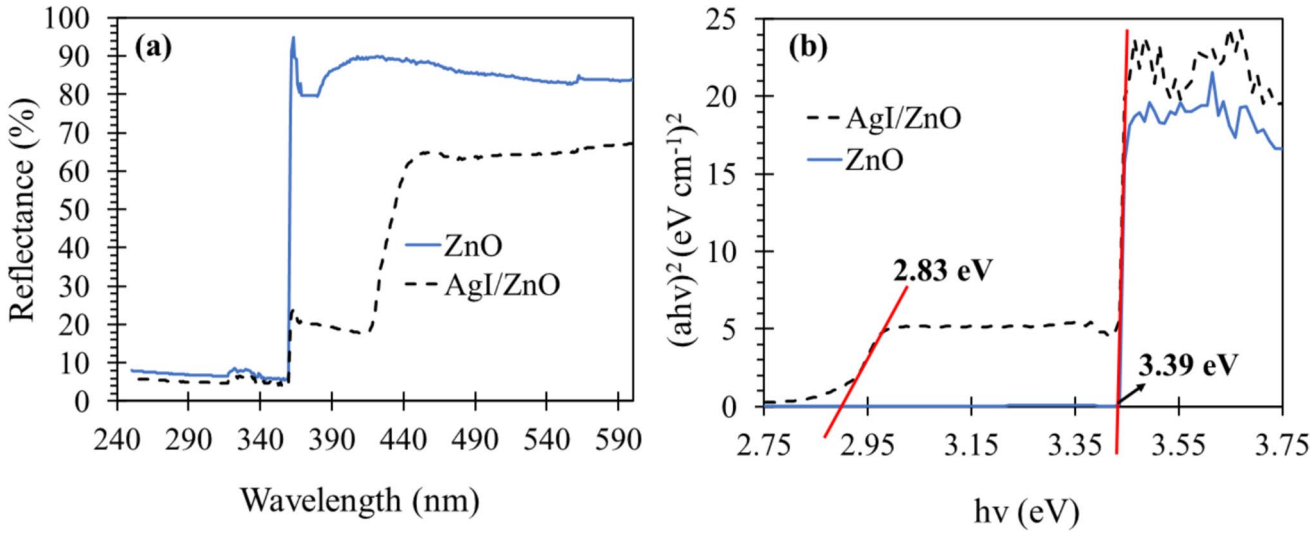

Fig. 3 **a** Reflectance Edge and **b** Tauc Plot of ZnO and AgI/ZnO

resulting in values of 3.39 and 2.83 eV, respectively, as depicted in Fig. 3b. As reported, the bandgap energy of AgI exhibited a lower bandgap than ZnO which is direct bandgap energy of ~ 1.378 eV (Amrani et al. 2008). Consequently, when AgI is incorporated onto ZnO, the composite's bandgap decreases, indicating enhanced light absorption. This modification promotes the generation of electron-hole pairs by mitigating photoelectron and hole recombination. The bandgap of the semiconductor was established using the Tauc plot method following Eq. 8. Thus, from the equation, the Tauc plot is plotted as $(\alpha hv)^2$ versus (hv). The value of bandgap was obtained by extrapolation of the linear part and the point meets the abscissa, thus, give the bandgap energy value (Jubu et al. 2022; Klein et al. 2023).

$$ahv = A\left(hv - E_g\right)^x \tag{8}$$

The VB and CB energies for ZnO and AgI/ZnO photocatalysts were determined using the Mulliken electronegativity formula. A summary of these findings is provided in Table 2. Equations 9–11 show the Mulliken electronegativity formula.

Table 2 The summary of the bandgap, valence band, and conduction band for ZnO and AgI/ZnO photocatalysts

Photocatalyst	Bandgap (eV)	Valence band (eV)	Conduction band (eV)
ZnO	3.39	0.30	− 0.20
AgI/ZnO	2.83	1.75	− 1.08

$$X = 1/2\left(E_{\mathrm{EA}} + E_{\mathrm{ion}}\right) \tag{9}$$

where the first ionization energy is (E_{ion}), the energy of atomic electron affinity is (E_{EA}), and X is a Mulliken electronegativity. Next, using Eq. 10, the (E_{CB}) was determined to get the CB:

$$E_{\mathrm{CB}} = X - E_C - 1/2\left(E_g\right) \tag{10}$$

where E_c is the energy of free electrons on the hydrogen scale (4.5 eV), and E_g is the energy bandgap. Equation 11

was used to determine E_{VB} from the photocatalyst's CB value and E_{CB} value.

$$E_{VB} = E_{CB} + E_g \quad (11)$$

Adsorption and photo-degradation studies of TC molecules by AgI/ZnO photocatalyst

Figure 4 illustrates the graph depicting the control test aimed at comparing the adsorption and photodegradation reactions. The results indicated that in the absence of any light source, only adsorption occurred, resulting in a marginal increase in TC concentration reduction, reaching only 19.15%. Conversely, when the catalyst was exposed to 150 W light for 90 min, a significantly higher degradation rate of 75.42% was observed. This highlights the crucial role of the light source in photocatalysis, providing the necessary energy to activate the catalyst and facilitate the desired chemical reactions. This approach aligns with previous studies, such as that conducted by Caniati et al. (2021) where similar control tests were employed to validate findings. Thus, this discovery emphasizes the indispensable requirement of light for activating the activity of the photocatalyst.

Effect of initial concentration of TC solution

Figure 5a portrays how the initial concentration of TC affects the photocatalyst's ability to degrade TC. The adsorption phase took place in darkness for 30 min, during which no degradation was observed. Over a 90 min period with light exposure, degradation rates of 72.17 and 83.45% were recorded for TC concentrations of 6 and 8 mg/L, respectively. According to first-order kinetics, lower concentrations are expected to yield degradation rates directly proportional to the substrate concentration, with the importance of catalytic sites being less significant in TC degradation. Raising the initial TC concentration to 10 mg/L achieved maximum degradation of 92.26% within the same duration. As elucidated by (Hasham et al. 2024), the generation of ·OH radicals on the photocatalyst's surface effectively broke down TC molecules. Consequently, higher concentrations necessitate more active species (·OH and $\cdot O_2^-$) for degradation. However, within the same timeframe, increasing the concentration to 12 and 14 mg/L resulted in degradation rates of 63.97 and 53.62%, respectively. As highlighted by Syahin et al. (2019), inadequate $\cdot O_2^-$ radicals at higher concentrations and the formation of intermediates that adsorb onto the catalyst surface contribute to slower degradation. In conclusion, the optimal initial concentration is 10 mg/L for 0.1 g of AgI/ZnO photocatalyst, emphasizing the significant influence of TC's initial concentration on photocatalysis reactions. Table 3 provides a summary of key parameters and photocatalytic performance compared with other studies, showcasing the superior degradation efficiency of AgI/ZnO, even with lower energy consumption.

Effect of Ag/ZnO dosage

Figure 5b depicts the degradation of TC at a concentration of 10 mg/L using varying amounts of catalyst, 0.1, 0.2, 0.3 and 0.4 g. Over a 90 min period, the degradation rates for TC were measured at 90.49, 81.48, 84.86, and 65.44%, respectively. These findings suggest that increasing the dosage of the catalyst leads to decreased degradation efficiency. As noted by Sawunyama et al.

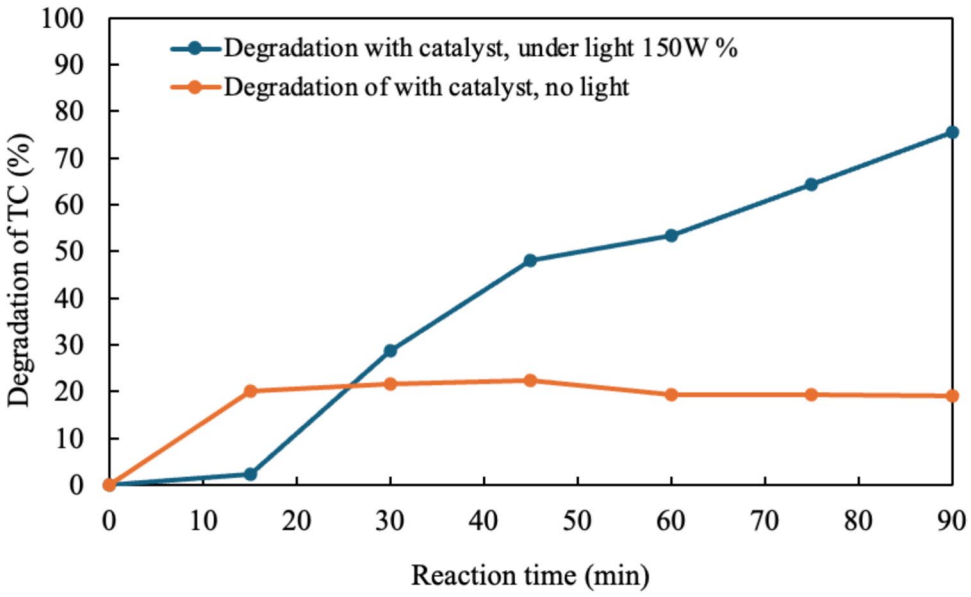

Fig. 4 Control test of the prepared AgI/ZnO photocatalyst on degradation of TC solution (Operating paramaters: 0.01 g of AgI/ZnO, 10 mg/L TC solutions at pH 9 within 90 min)

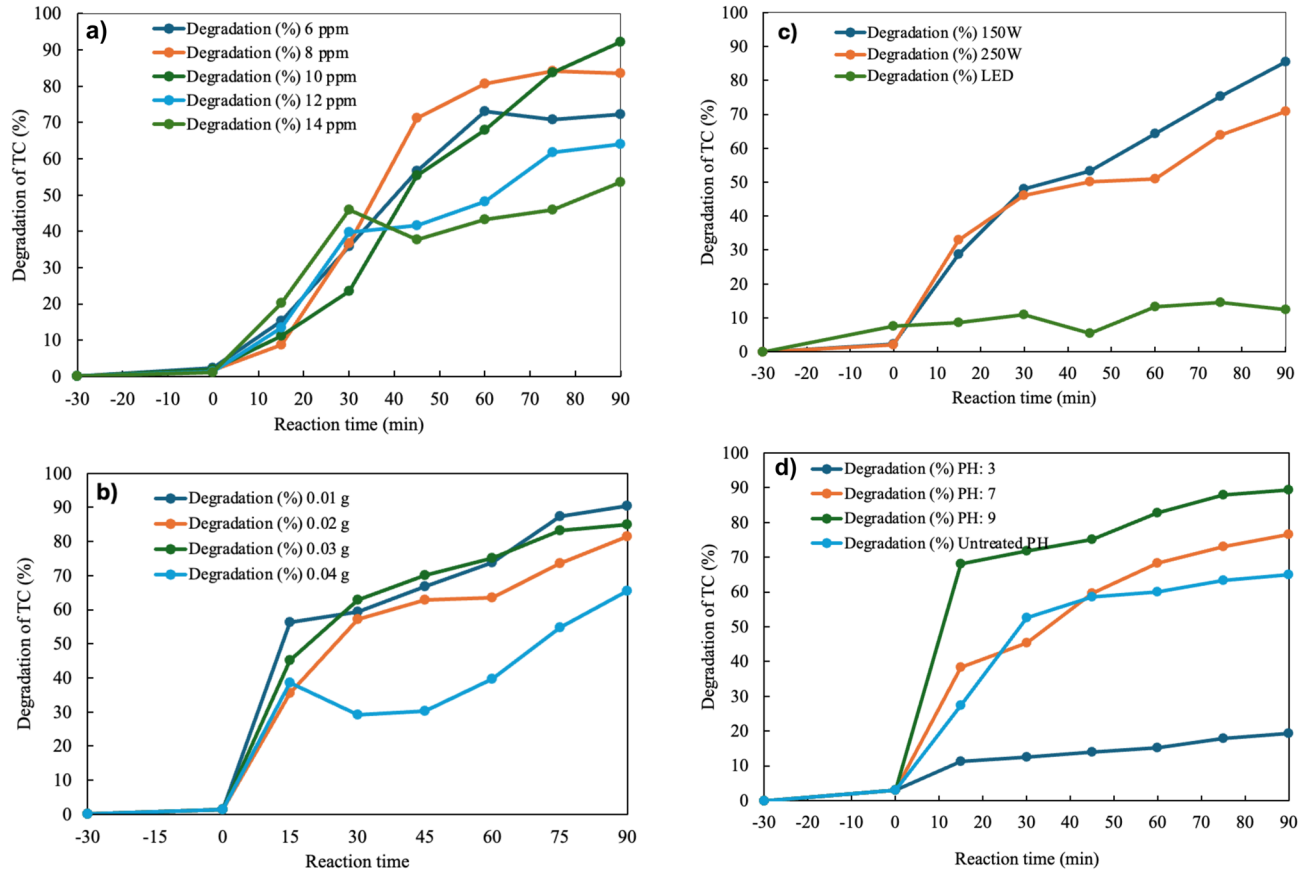

Fig. 5 **a** The effect of initial concentration of TC solution. (Reaction condition: 0.1 g of AgI/ZnO catalyst dosage, 100 mL of TC solution, untreated pH, and 250-W metal halide lamp), **b** The effect of catalyst dosage of TC solution. (Reaction condition: 10 mg/L of AgI/ZnO initial concentration, 100 mL of TC solution, untreated pH, and 250-W metal halide lamp), **c** The effect of light intensity of TC solution. (Reaction condition: 10 mg/L of AgI/ZnO initial concentration, 0.01 g of catalyst, 100 mL of TC solution, and untreated pH), **d** The effect of pH of TC solution. (Reaction condition: 10 mg/L of AgI/ZnO initial concentration, 0.01 g of catalyst, 100 mL of TC solution, and 150-W metal halide lamp)

(2023), higher doses of AgI/ZnO may induce turbidity in the solution, causing interruptions in light transmission during the reaction, thereby affecting the efficacy of TC removal. Furthermore, the aggregation of nanocomposites at higher catalyst doses, influenced by the magnetic properties of synthesized nano-catalysts, can result in unfavourable light scattering and reduced light penetration into the solution, ultimately diminishing photocatalytic activity (Hayat et al. 2011). While at very low concentrations below than 0.1 g, the photocatalyst may degrade faster due to the limited number of active sites, which may become deactivated by impurities or intermediates (Majumdar and Pal, 2020; Mashuri et al. 2020). Based on these observations, it was decided that in subsequent photocatalytic degradation trials, the amount of AgI/ZnO would be maintained at the optimal value of 0.01 g.

Effect of irradiation intensity

The study investigated the effect of light intensity on photocatalytic performance using various types of lamps with differing intensities over a 90 min period. According to Fig. 5c, TC degradation was most significant when employing 150-W metal halide lamps compared to both 250-W metal halide lamps and LED lamps. The excessively high excitation intensities could lead to congestion of charge carriers, affecting the recombination mechanism and potentially reducing degradation rates (Schneider and Curti 2023). Therefore, increasing light intensity excessively may not effectively enhance electron utilization, and not all catalysts can withstand such high light intensities during photocatalytic reactions. Thus, it is essential for incident light to provide a photon energy threshold conducive to promoting

Table 3 Comparison previously reported work on various pollutant degradation using ZnO-based photocatalyst

Pollutant	Catalyst	Bandgap (eV)	Light sources	Optimized parameter degradation efficiency			Degradation (%)	Ref
				Concentration (mg/L)	Catalyst dosage	Time (min)		
Tetracycline	ZnO/Dy	2.47	500-W Xenon lamp	20	25 mg	120	74.19	(Dhiman et al. 2023)
Ciprofloxacin	ZnO-Ag-Graphitic	2.95	24-W UV lamp (λ = 254 nm)	5	0.3 g/L	60	98	(Roy et al. 2023)
Naproxen	Ag/AgI/ZnO (75% Ag)	1.93	300-W Xenon lamp	2	10 mg	60	100	(Ding et al. 2021)
Tetracycline	Ag/ZnO@BC	3.8	500-W Xenon lamp	50	10 mg	60	70.3	(Hosny et al. 2022)
Oxytetracycline	Ag/ZnO	3.0	Sunlight	10	50 mg	240	99	(Wannakan et al. 2022)
Tetracycline	CDots/Ag/ZnO	3.08	150-W Xenon lamp	30	15 mg	60	96	(Li et al. 2021)
Tetracycline	Ag/ZnO/$InVO_4$	2.31	500-W Xenon lamp	10	30 mg	120	88.6	(Ou et al. 2024)
Ciprofloxacin	AgI/ZnO	2.84	300-W Xenon lamp	10	20 mg	120	99.7	(Wu et al. 2021)
Tetracycline	**AgI/ZnO**	**2.83**	**150-W metal halide**	**10**	**10 mg**	**90**	**89.38**	**Present study**

photocatalysis. Consequently, the study determined that the optimal light intensity was a 150-W metal halide lamp, which will be employed in all subsequent reactions.

Effect of pH of TC solution

The pH level is a major component that affects how quickly some organic compound pollutants degrade because it determines the catalyst's surface charge characteristics and the size of the aggregates it forms (Sapawe et al. 2013b). The Fig. 5d illustrates the impact of different pH levels on TC solutions, including pH 3 (acidic), pH 7 (neutral), pH 9 (basic), and untreated pH (no pH adjustment) for 90 min reaction. The order of the photocatalytic degradation efficiencies of TC at various pH levels was pH9 (89.38%) > pH7 (76.52%) > Untreated pH (64.92%) > pH3 (19.35%). The results indicate that a higher pH solution (more basic) exhibited the highest degradation since there were more hydroxide ions accessible on the photocatalyst surface and developing of hydroxyl radicals that contributed to the quicker breakdown of TC (Anyou et al. 2023). This trend is consistent with previous studies (Sawunyama et al. 2023), which reported that TC undergoes favourable photocatalysis in alkaline conditions, likely due to the strong interaction between TC^- and ·OH radicals. As a result, TC absorbs more photons, enhancing photocatalysis. However, increasing the pH beyond a certain threshold does not significantly improve degradation efficiency. While higher pH levels increase OH^- availability, leading to greater hydroxyl radical production, excessively high pH can result in the formation of stable intermediates that are resistant to further breakdown. Additionally, very high pH may cause photocatalyst particles to agglomerate, reducing the surface area available for catalytic reactions.

However, the lowest degradation rate can be seen in the TC solution at pH 3 (19.35%), which is in acidic conditions. According to (Fiaz et al. 2021b), ZnO not being acid-resistant, which explains why TC degrades slowly in acidic environments. It may also be explained by the repellent force that exists between the positively charged catalyst and protonated TC. Because the reduced surface area of the photocatalysts results from nanoparticle aggregation in acidic environments, some metal oxide nanoparticles are found to have low photocatalytic performance. Overall, at high pH (7.05–9.67), the degradation of TC molecules can be considered environmentally friendly as freer ·OH radicals are produced as shown in the Eq. 12 below. Additionally, AgI can lead to secondary pollution; however, an alkaline pH environment helps mitigate this issue. At higher pH, silver ion (Ag^+) exhibits reduced solubility due to the formation of silver hydroxide (AgOH), which can precipitate as insoluble silver oxide (Ag_2O), minimizing Ag^+ leaching into the environment. Furthermore, AgI remains stable in alkaline conditions, as iodide ions (I^-) are less likely to dissociate from the AgI complex, ensuring that AgI stays bound within the ZnO matrix. Alkaline conditions are also less corrosive

to the photocatalyst compared to acidic environments, where material breakdown and dissolution are more common (Lu et al. 2024). Therefore, field applications will require systems capable of maintaining sufficient alkalinity to ensure optimal performance as reported by Wang et al. (2024) and Seyyedbagheri et al. (2023).

$$OH^- + h^+ \rightarrow \cdot OH \quad (12)$$

Proposed mechanism of degradation TC molecules by AgI/ZnO photocatalyst

The radical scavenging experiments were conducted under optimized reaction conditions for the degradation process to identify the primary reactive species involved in the AgI/ZnO photocatalytic degradation of TC. As depicted in Fig. 6a, in the absence of scavenger reagents, the degradation rate of TC reached 89.38%. However, the introduction of additional scavenger reagents disrupted the photocatalytic reaction by capturing the reactive species. Specifically, the presence of scavenger agents such as p-BQ, EDTA, $AgNO_3$, and IPA, which trap $\cdot O_2^-$, h^+, e^-, and OH· species respectively, hindered the TC degradation process. The presence of EDTA and IPA resulted in reductions in TC degradation to 65.9 and 79.43% respectively, indicating limited involvement of h^+ and $OH^·$ in the photodegradation reactions. Conversely, the addition of $AgNO_3$ and p-BQ reagent trap e^- and $\cdot O_2^-$ respectively, significantly slowed down the degradation rate to 34.86 and 44.54%, highlighting the pivotal role of e^- and $\cdot O_2^-$ as primary active species in the photodegradation system. According to Zhu et al. (2020), the $\cdot O_2^-$ radical is generated through the reaction between e^- and dispersed O_2 molecules, which can be captured by p-BQ, highlighting its significance in the photocatalytic breakdown of TC. In summary, h^+ and ·OH contribute minimally to the degradation of TC molecules, whereas e^- and $\cdot O_2^-$ radicals play major roles in the process.

Based on the findings from scavenger experimental and analytical investigations, a plausible photo-degradation mechanism is proposed in Fig. 6b. The process of photocatalysis for TC comprises two distinct phases: a homogeneous photo-induced phase and a heterogeneous indirect photolysis phase. In the homogeneous photo-induced phase, TC is exposed to visible light irradiation, leading to the

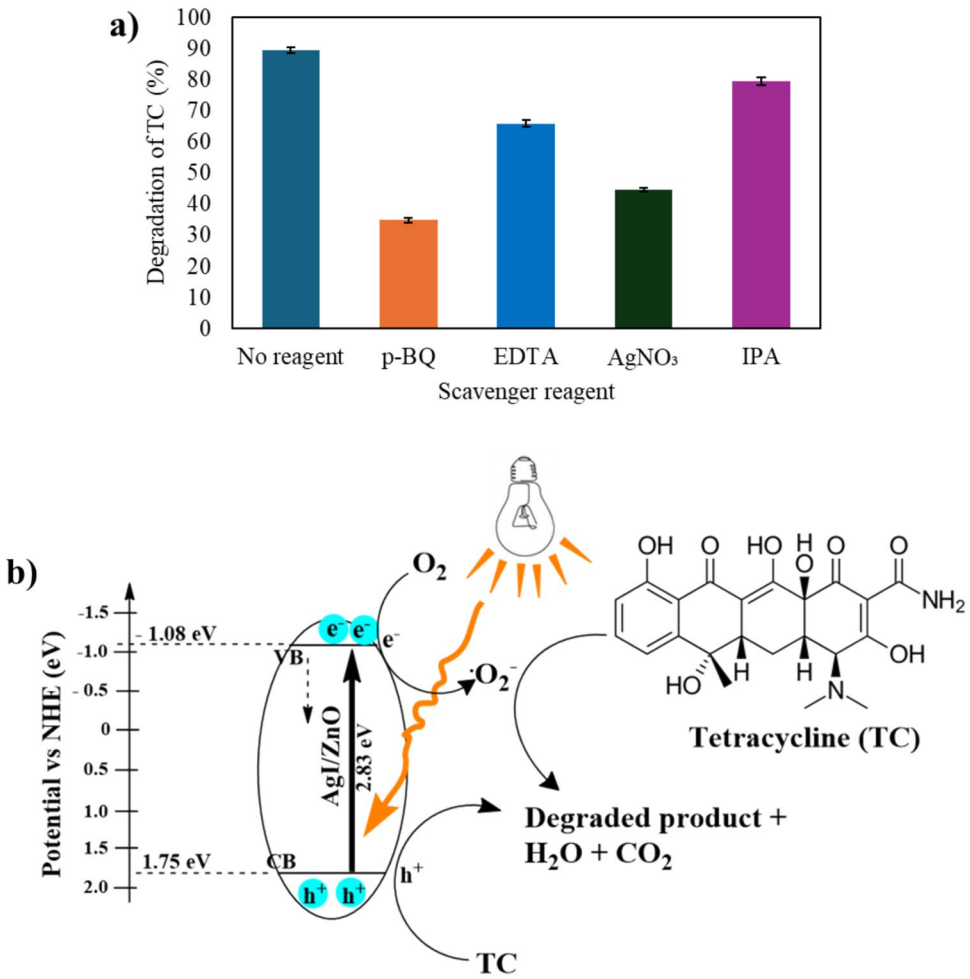

Fig. 6 **a** Radical scavenger test over AgI/ZnO in the degradation TC. (Reaction condition: 10 mg/L of AgI/ZnO initial concentration, 0.01 g of catalyst, pH 9 of TC solution, and 150-W metal halide lamp) and **b** proposed mechanism of TC catalysed by AgI/ZnO photocatalyst

deprotonation of TC (TC^-). Subsequently, TC^- undergoes decarboxylation, facilitating bond cleavage within the TC molecule and enhancing its reactivity towards free radicals before engaging in free radical reactions. The bandgap energy of AgI/ZnO is 2.83 eV, allowing direct excitation to generate photoinduced e^- and h^+ pairs under visible light irradiation (Ding et al. 2021; Sawunyama et al. 2023).

In the heterogeneous phase induced by ROS, it is theoretically postulated that the redox potential of $O_2/\cdot O_2^-$ (−0.33 eV) is less negative than that of AgI/ZnO (−1.08 eV), allowing e^- in AgI/ZnO_{CB} to be captured by dissolved molecular O_2 to produce $\cdot O_2^-$, which can degrade TC. Some excited e^- in AgI/ZnO_{CB} may revert to the AgI/ZnO_{VB} and recombine with h^+. However, due to the lower redox potential of the AgI/ZnO_{VB} (+1.75 eV) compared to $\cdot OH/OH^-$ (+2.38 eV) and $\cdot OH/H_2O$ (+2.72 eV), AgI/ZnO cannot oxidize OH^- and H_2O to ·OH effectively, as evidenced by scavenger tests showing minimal contribution of ·OH during the reaction. Additionally, Ding et al. mentioned that in alkaline conditions, TC^- predominates in the system, leading to preferential reaction of h^+ in the VB of AgI/ZnO with a large quantity of TC^- rather than with OH^-, given TC^-'s higher reactivity in a photo-induced reaction system. In summary, the photocatalytic reaction can be described by the following equations (Eq. 13–17):

$$TC\left(C_{22}H_{24}N_2O_8\right) \rightarrow TC^-\left(C_{22}H_{23}N_2O_8\right)^- + H^+ \quad (13)$$

$$TC^-\left(C_{22}H_{23}O_8\right)^- + H^+ \rightarrow \text{By - product}\left(C_{22}H_{24}O_6\right) + CO_2 \quad (14)$$

$$AgI/ZnO + hv \rightarrow AgI/ZnO\ (e^- + h^+) \quad (15)$$

$$AgI/ZnO\ (e^-) + O_2 \rightarrow AgI/ZnO + \cdot O_2^- \quad (16)$$

$$\cdot O_2^-/h^+ + \text{by - products}\ \left(C_{22}H_{24}O_6\right) \rightarrow \text{Degradation products} + H_2O + CO_2 \quad (17)$$

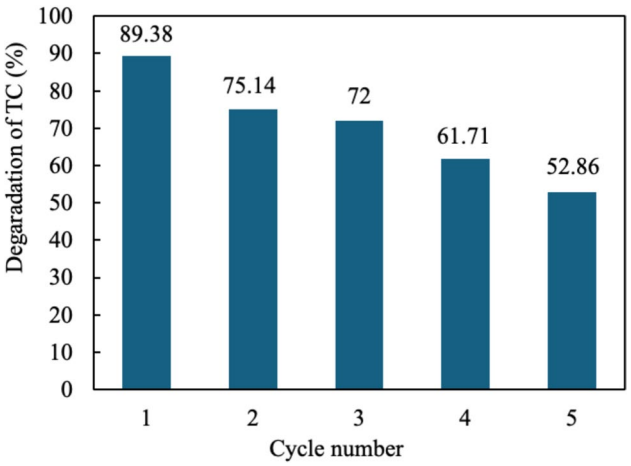

Fig. 7 The cycle life of the AgI/ZnO catalyst. (Reaction condition: 10 mg/L of AgI/ZnO initial concentration, 0.01 g of catalyst, pH 9 of TC solution, and 150-W metal halide lamp)

Recyclability of the AgI/ZnO catalyst

The reusability test revealed (Fig. 7) that the AgI/ZnO catalyst exhibits promising photostability over a 90-min duration. In successive runs, the degradation percentages of TC were recorded as 89.38, 75.14, 72, 61.71, and 52.86%, respectively. This suggests that the photocatalytic activity of AgI/ZnO composites displays favourable reusability, indicating excellent stability of the catalyst. Moreover, the electrostatic ionic bonding from AgI and semiconducting behaviour from ZnO proposed a key factor that contributing to the stability and reusability in degradation TC (Ding et al. 2021). In essence, it retains its efficacy over time and can be utilized repeatedly without notable degradation.

Conclusion

The degradation of organic contaminants through photocatalysis is anticipated to be both effective and efficient. In this study, the AgI/ZnO composite photocatalyst was successfully synthesized using photo-deposition techniques. XRD analysis revealed crystalline characteristics, displaying distinct peaks for both ZnO and AgI. FESEM images depicted hexagonal wurtzite ZnO flowers supported by cubic AgI nanoparticles ranging in size from 70 to 80 nm. HRTEM analysis, conducted using ImageJ software, measured the interplanar crystal spacing (d) of AgI (110) particles at 0.2412 nm and ZnO (002) at 0.337 nm. Additionally, the surface area of AgI/ZnO exhibited higher values compared to pure ZnO, and its bandgap of 2.38 eV (VB 1.75 eV and CB − 1.08 eV) rendered it suitable for degrading TC under visible light. The incorporation of AgI with ZnO improved charge separation and enhanced photocatalytic efficiency, contributing to more effective TC degradation. Optimization experiments demonstrated that, with 0.01 g of AgI/ZnO, 10 mg/L TC solutions at pH 9 could be degraded within 90 min using a 150-W metal halide light source. In contrast, TC degradation without light exposure was limited to 19.15% (adsorption) but increased significantly to 89.392% with photocatalysis (degradation). Moreover, the AgI/ZnO composite exhibited good reusability, maintaining up to 52.86% degradation over five cycles. e^- and $\cdot O_2^-$ radicals were identified as the major species involved in the photocatalytic process. Looking ahead, future work could focus on minimizing the release of AgI and degraded tetracycline by exploring non-toxic co-catalysts or surface passivation

techniques to reduce Ag^+ leaching. Additionally, post-treatment methods such as adsorbents or filtration systems could further enhance environmental safety and applicability in field conditions. In conclusion, the discovered AgI/ZnO photocatalyst demonstrated excellent activity under visible light, effectively degrading TC solutions, and holds promise for further investigation with various organic pollutants.

Acknowledgements The authors would like to thank the Universiti Teknologi MARA (UiTM) for the University Internal Research Grant File No. 600-RMC/GIP 5/3 (004/2023) and Faculty of Applied Science for laboratory facilities and funding provided.

Author contributions Auni Mahirah Muhamad Hissam: First author, writing- original draft, analysis, investigation, methodology. Salma Izati Sinar Mashuri: Supervision, methodology, data curation, review and editing. Nor Fadilah Chayed: Supervision, methodology, data curation. Nur Hazirah Rozali Annuar: Supervision, visualization. Nurul Asikin-Mijan: Data curation. Siti Fadhilah Ibrahim: Review and editing. Nur Hidayati Othman: Data curation. Abdulkareem Ghassan Alsultan: Data curation. Tan Yie Hua: Data curation. Umer Rashid: Supervision, visualization. Taufiq Yap Yun Hin: Supervision, visualization. Mohd Lokman Ibrahim: Supervision, resources, funding acquisition, review and editing.

Funding Open access funding provided by The Ministry of Higher Education Malaysia and Universiti Teknologi MARA.

Declarations

Conflict of interest The authors declare that they have no known competing financial interests or personal relationships that could have appeared to influence the work reported in this paper.

Ethical approval This article does not contain any studies with human participant or animal performed by any of the authors.

References

Ahmad F, Zhu D, Sun J (2021) Environmental fate of tetracycline antibiotics: degradation pathway mechanisms, challenges, and perspectives. Environ Sci Eur 33(1):64

Ahmed MA, Mohamed AA (2023) Recent progress in semiconductor/graphene photocatalysts: synthesis, photocatalytic applications, and challenges. RSC Adv 13(1):421–439

Amangelsin Y, Semenova Y, Dadar M, Aljofan M, Bjørklund G (2023) The impact of tetracycline pollution on the aquatic environment and removal strategies. Antibiotics (Basel) 12(3):440

Amiruddin MI, Mashuri SIS, Mutalib AAA, Chayed NF, Rashid U and Ibrahim ML (2021). Potential of advanced photocatalytic technology for biodiesel production from waste oil. In: Advanced technology for the conversion of waste into fuels and chemicals (pp 49–76). Woodhead Publishing

Arjmand F, Golshani Z, Fatemi SJ, Maghsoudi S, Naeimi A, Hosseini SMA (2022) The lead-free perovskite solar cells with the green synthesized BiI3 and AgI nanoparticles using *Vitex agnus-castus* plant extract for HTM-free and carbon-based solar cells. J Mater Res Technol 18:1922–1933

Azqandi M, Shahryari T, Fanaei F, Nasseh N (2023) Green construction of magnetic $MnFe_2O_4$/ZIF-8 nanocomposite utilizing extract of *Melissa officinalis* plant for the photo-degradation of tetracycline under UV illumination. Catal Commun 185:106798

Boxi SS (2024). Degradation of organic compounds in aqueous media using semiconductor nanomaterials. Univ J Green Chem, pp 96–105

Cao J, Ouyang M, Xu C, Li H, Chen Z, Chen L, Xu D (2024) Ultrafast sensitive colorimetric detection of cyanide based on dissolving AgI on Au-AgI heterodimeric nanoparticles via UV–vis spectroscopy and single nanoparticle imaging. Sens Actuators B Chem 410:135635

Chayed NF, Mashuri SIS, Abidin NSIZ, Kasim MF, Kaus NHM, Mastuli MS, Rashid U, Ibrahim ML (2023) Photocatalytic degradation of ofloxacin antibiotic by g-C_3N_4/ZnO nanocomposite under visible light irradiation. Malays J Anal Sci 27:1326–1336

Dhiman P, Rana G, Kumar A, Dawi EA, Sharma G (2023) Rare earth doped ZnO nanoparticles as spintronics and photo catalyst for degradation of pollutants. Molecules (Basel) 28(6):2838

Ding C, Fu K, Pan Y, Liu J, Deng H, Shi J (2020) Comparison of Ag and AgI-modified ZnO as heterogeneous photocatalysts for simulated sunlight driven photodegradation of metronidazole. Catalysts (Basel) 10(9):1097

Ding C, Fu K, Wu M, Gong S, Liu J, Shi J, Deng H (2021) Photocatalytic performance and mechanism of AgI/Ag/ZnO composites as catalysts for the visible-light-driven degradation of naproxen. J Photochem Photobiol A Chem 414:113283

Doosti M, Jahanshahi R, Laleh S, Sobhani S, Sansano JM (2022) Solar light induced photocatalytic degradation of tetracycline in the presence of ZnO/4/Co_3O_4 as a new and highly efficient magnetically separable photocatalyst. Front Chem 10:1013349

Drwal K, Miecznikowski K, Krasnodębska-Ostręga B (2022) Photoactive materials for decomposition of organic matter prior to water analysis—a review containing original research. Catalysts (Basel) 12(6):616

Escaliante LC, Rocha KDO, Silva JHDD (2021) Stability of the photocatalytic activity of TiO_2 deposited by reactive sputtering. Mater Res 24(Suppl 1):e20210051. https://doi.org/10.1590/1980-5373-mr-2021-0051

Ghattavi S, Nezamzadeh-Ejhieh A (2019) A brief study on the boosted photocatalytic activity of AgI/WO_3/ZnO in the degradation of methylene blue under visible light irradiation. Desalin Water Treat 166:92–104

Gokul T, Kumar KR, Veeramanikandan V, Arun A, Balaji P, Faggio C (2023) Impact of particulate pollution on aquatic invertebrates. Environ Toxicol Pharmacol 100:104146

Güell F, Galdámez-Martínez A, Martínez-Alanis PR, Catto AC, da Silva LF, Mastelaro VR, Santana G, Dutt A (2023) ZnO-based nanomaterials approach for photocatalytic and sensing applications: recent progress and trends. Mater Adv 4(17):3685–3707

Guo Y, Fu X, Xie Y, Zhu L, Liu R, Liu L (2022) Synthesis of Ag/ZnO nanocomposites with enhanced visible photocatalytic performance. Opt Mater 133:112980

Hasham FM, Naderi A, Moradi M, Kalantary RR (2024) Enhanced tetracycline degradation with TiO2/natural pyrite S-scheme photocatalyst. Sci Rep 14(1):4954

Hosny M, Fawzy M, Eltaweil AS (2022) Green synthesis of bimetallic Ag/ZnO@ biohar nanocomposite for photocatalytic degradation of tetracycline, antibacterial and antioxidant activities. Sci Rep 12(1):7316

Hudandini M, Puri NR, Winardi S, Widiyastuti W, Shimada M, Kusdianto K (2022) Photocatalytic activity of ZnO/Ag nanoparticles fabricated by a spray pyrolysis method with different O_2: N_2 carrier gas ratios and Ag contents. Catalysts 12(11):1374

Ibrahim SF, Shohaimi NAM, Ibrahim ML et al (2023) Photo-esterification of waste cooking oil using a novel nanocatalyst TiO_2 impregnated with empty fruit bunches ash heterogeneous catalyst. Malays J Anal Sci 27:586–599

Ibrahim SF, Shohaimi NAM, Hir ZAM, Mastuli MS, Hin TYY, Ibrahim ML (2024) Efficient photocatalytic esterification of waste cooking oil over empty fruit bunches ash-supported TiO_2. Iran J Catal (IJC) 14(3):1–16

Jia K, Liu G, Lang DN, Chen SF, Yang C, Wu RL, Wang W, Wang JD (2022) Degradation of tetracycline by visible light over ZnO nanophotocatalyst. J Taiwan Inst Chem Eng 136:104422. https://doi.org/10.1016/j.jtice.2022.104422

Jubu PR, Obaseki OS, Nathan-Abutu A, Yam FK, Yusof Y, Ochang MB (2022) Dispensability of the conventional Tauc's plot for accurate bandgap determination from UV–vis optical diffuse reflectance data. Results Opt 9:100273. https://doi.org/10.1016/j.rio.2022.100273

Kadem AJ, Tan ZM, Suntharam NM, Pung SY, Ramakrishnan S (2023) Synthesis of CuO, ZnO and SnO_2 coupled TiO_2 photocatalyst particles for enhanced photodegradation of rhodamine B dye. Bull Chem React Eng Catal. https://doi.org/10.9767/bcrec.19532

Khalit WNAW, Marliza TS, Asikin-Mijan N, Gamal MS, Saiman MI, Ibrahim ML, Taufiq-Yap YH (2020) Development of bimetallic nickel-based catalysts supported on activated carbon for green fuel production. RSC Adv 10(61):37218–37232

Klein J, Kampermann L, Mockenhaupt B, Behrens M, Strunk J, Bacher G (2023) Limitations of the Tauc plot method. Adv Funct Mater 33(47):2304523

Li T, Liu Y, Li M, Jiang J, Gao J, Dong S (2021) Fabrication of oxygen defect-rich pencil-like ZnO nanorods with CDots and Ag co-enhanced photocatalytic activity for tetracycline hydrochloride degradation. Sep Purif Technol 266:118605. https://doi.org/10.1016/j.seppur.2021.118605

Li X, Wei H, Song T, Lu H, Wang X (2023) A review of the photocatalytic degradation of organic pollutants in water by modified TiO_2. Water Sci Technol 88(6):1495–1507

Liu J, Chen J, Wu Z, Zhu K, Wang J, Li Z, Tai G, Liu X, Lu S (2021) Enhanced visible-light photocatalytic performances of ZnO through loading AgI and coupling piezo-photocatalysis. J Alloys Compd 852:156848. https://doi.org/10.1016/j.jallcom.2020.156848

Liu X, Wang H, Wang C, Zhao L, Pan H, Liu Y, Liang L, Zhao C, Huang S (2024) Self-endowed magnetic photocatalysts derived from iron-rich sludge and its recycling in photocatalytic process for tetracycline degradation. Bioresour Technol 395:130357. https://doi.org/10.1016/j.biortech.2024.130357

Lu H, Wang X, Cong Q, Chen X, Li Q, Li X, Zhong S, Deng H, Yan B (2024) Research progress on the degradation of organic pollutants in water by activated persulfate using biochar-loaded nano zero-valent iron. Molecules 29(5):1130

Luu TVH, Nguyen HYX, Nguyen QT, Nguyen QB, Nguyen THC, Pham NC, Nguyen XD, Nguyen TK, Dao NN (2024) Enhanced photocatalytic performance of ZnO under visible light by co-doping of Ta and C using hydrothermal method. RSC Adv 14(18):12954–12965

Mao T, Liu M, Lin L, Cheng Y, Fang C (2022) A study on doping and compound of zinc oxide photocatalysts. Polymers 14(21):4484

Mashuri SIS, Ibrahim ML, Kasim MF, Mastuli MS, Rashid U, Abdullah AH, Islam A, Asikin Mijan N, Tan YH, Mansir N, Mohd Kaus NH (2020) Photocatalysis for organic wastewater treatment: from the basis to current challenges for society. Catalysts 10(11):1260

Mashuri SIS, Kasim MF, Kaus NHM, Tan YH, Islam A, Rashid U, Asikin-Mijan N, Andas J, Taufiq-Yap YH, Yaakob MK, Ismail WINW (2023) Photo-response range extension of Z-scheme ZnO/CdS for LED-light-driven photo-active catalyst. Renew Sustain Energy Rev 184:113602. https://doi.org/10.1016/j.rser.2023.113602

Mohd Kaus NH, Ibrahim ML, Imam SS, Mashuri SIS and Kumar Y (2022). Efficient visible-light-driven perovskites photocatalysis: design, modification and application. In: Green photocatalytic semiconductors: recent advances and applications, pp.357–398

Mohd Shohaimi NA, Adnan NK, Ibrahim SF (2024) Photoesterification of waste cooking oil using ZnO doped empty fruit bunches ash heterogeneous catalyst. Recent Innov Chem Eng (Formerly Recent Pat Chem Eng) 17(2):119–133

Moiz MA, Mumtaz A, Salman M, Husain SW, Baluch AH, Ramzan M (2021) Band gap engineering of ZnO via transition metal doping: an ab initio study. Chem Phys Lett 781:138979. https://doi.org/10.1016/j.cplett.2021.138979

Nguyen VH, Smith SM, Wantala K, Kajitvichyanukul P (2020) Photocatalytic remediation of persistent organic pollutants (POPs): a review. Arab J Chem 13(11):8309–8337

Ou X, Zhao K, Chen P, Xia C, Wei M, Zhang M, Wang Y (2024) Visible-light responsive Ag-doped ZnO/InVO4 composite photocatalyst for efficient degradation of tetracycline and inactivate *E. coli*. J Alloys Compd. https://doi.org/10.1016/j.jallcom.2024.175230

Pavel M, Anastasescu C, State RN, Vasile A, Papa F, Balint I (2023) Photocatalytic degradation of organic and inorganic pollutants to harmless end products: assessment of practical application potential for water and air cleaning. Catalysts 13(2):380

Pham GT, Vu HT, Pham TT, Thanh NN, Tran HQ, Doan HV, Nguyen MB (2023) Exploring the potential of ZnO–Ag@ AgBr/SBA-15 Z-scheme heterostructure for efficient wastewater treatment: synthesis, characterization, and real-world applications. RSC Adv 13(18):12402–12410

Rajput RB, Shaikh R, Sawant J, Kale RB (2022) Recent developments in ZnO-based heterostructures as photoelectrocatalysts for wastewater treatment: a review. Environ Adv 9:100264. https://doi.org/10.1016/j.envadv.2022.100264

Ramírez AE, Montero-Muñoz M, López LL, Ramos-Ibarra JE, Coaquira JA, Heinrichs B, Páez CA (2021) Significantly enhancement of sunlight photocatalytic performance of ZnO by doping with transition metal oxides. Sci Rep 11(1):2804

Roy TS, Akter S, Fahim MR, Gafur MA, Ferdous T (2023) Incorporation of Ag-doped ZnO nanorod through Graphite hybridization: effective approach for degradation of ciprofloxacin. Heliyon. https://doi.org/10.1016/j.heliyon.2023.e13130

Sawunyama L, Oyewo O, Onwudiwe DC, Makgato SS (2023) Photocatalytic degradation of tetracycline using surface defective black TiO2–ZnO heterojunction photocatalyst under visible light. Heliyon. https://doi.org/10.1016/j.heliyon.2023.e21423

Sayyed MI, Abdo MA, Ali HE, Sadeq MS (2022) Transparent and radiation shielding effective Na_2O–CrO_3 borate glasses via AgI additives. Ceram Int 48(20):30817–30825

Schneider J, Curti M (2023) Spectroscopic and kinetic characterization of photogenerated charge carriers in photocatalysts. Photochem Photobiol Sci 22(1):195–217

Semeraro P, Bettini S, Sawalha S, Pal S, Licciulli A, Marzo F, Lovergine N, Valli L, Giancane G (2020) Photocatalytic degradation of tetracycline by ZnO/γ-Fe_2O_3 paramagnetic nanocomposite material. Nanomaterials 10(8):1458

Seyyedbagheri H, Alizadeh R, Mirzayi B (2023) A novel heterostructure ZnO/PbBiO2Cl as a type-II photocatalyst for persulfate

activation in tetracycline degradation under visible light. J Mol Liq 383:122067. https://doi.org/10.1016/j.molliq.2023.122067
Taghizadeh MT, Siyahi V, Ashassi-Sorkhabi H, Zarrini G (2020) ZnO, AgCl and AgCl/ZnO nanocomposites incorporated chitosan in the form of hydrogel beads for photocatalytic degradation of MB, *E. coli* and *S. aureus*. Int J Biol Macromol 147:1018–1028
Talreja N, Ashfaq M, Chauhan D, Mera AC, Rodríguez CA, Mangalaraja RV (2021) A Zn-doped BiOI microsponge-based photocatalyst material for complete photodegradation of environmental contaminants. New J Chem 45(39):18412–18420
Tang J, Okabe T, Nishimura K, Sciazko A, Zhang H, Shikazono N (2024) Frost growth on silver iodide (AgI) stripe patterned surface under condensation frosting condition. Int J Heat Mass Transfer 235:126237. https://doi.org/10.1016/j.ijheatmasstransfer.2024.126237
Tegenaw AB, Yimer AA, Beyene TT (2023) Boosting the photocatalytic activity of ZnO-NPs through the incorporation of C-dot and preparation of nanocomposite materials. Heliyon. https://doi.org/10.1016/j.heliyon.2023.e20717
Tofanello A, Belleti E, Brito AM, Nantes-Cardoso IL (2021) Photodegradation of ciprofloxacin-zinc complexes produced at the interface of ZnO and Cu-doped ZnO crystals. Mater Res 24(6):e20210198. https://doi.org/10.1590/1980-5373-mr-2021-0198
Wang X, Wang X, Zhang H, Zhang J, Li Z, Wang X, Xu J, Cao D, Li J, Lu C (2024) Photothermal-assisted photocatalytic degradation of tetracycline in simulated natural water by $BiVO_4$/$CuBi_2O_4$ Z-scheme heterojunction: mechanisms insight, degradation pathways and toxicity assessment. Process Saf Environ Prot. https://doi.org/10.1016/j.psep.2024.06.042
Wannakan K, Khansamrit K, Senasu T, Chankhanittha T, Nanan S (2022) Ag-modified ZnO for degradation of oxytetracycline antibiotic and reactive red azo dye. Antibiotics 11(11):1590
Wu X, Zhang Y, Wu H, Guo J, Wu K, Zhang L (2021) Facile synthesis of multi-shelled AgI/ZnO composite as Z-scheme photocatalyst for efficient ciprofloxacin degradation and H 2 production. J Mater Sci Mater Electron 32:26241–26257
Xie A, Jin M, Zhu J, Zhou Q, Fu L, Wu W (2023) Photocatalytic technologies for transformation and degradation of microplastics in the environment: current achievements and future prospects. Catalysts 13(5):846
You CS, Jung SC (2024) Photo-catalytic destruction of tetracycline antibiotics using terbium and manganese co-precipitated TiO_2 photocatalyst. J Environ Chem Eng 12(1):111666. https://doi.org/10.1016/j.jece.2023.111666
Zamri MSFA, Sapawe N (2019) Kinetic study on photocatalytic degradation of phenol using green electrosynthesized TiO2 nanoparticles. Mater Today Proc 19:1261–1266. https://doi.org/10.1016/j.matpr.2019.11.131
Zarezadeh S, Habibi-Yangjeh A, Mousavi M, Ghosh S (2020) Novel ZnO/Ag_3PO_4/AgI photocatalysts: preparation, characterization, and the excellent visible-light photocatalytic performances. Mater Sci Semicond Process 119:105229. https://doi.org/10.1016/j.mssp.2020.105229
Zhan L, Xia Z, Xu Z, Xie B (2021) Study on the remediation of tetracycline antibiotics and roxarsone contaminated soil. Environ Pollut 271:116312
Zhou T, Zhang H, Ma X, Zhang X, Zhu Y, Zhang A, Cao Y, Yang P (2020) Construction of AgI/Bi_2MoO_6/AgBi (MoO_4) 2 multi-heterostructure composite nanosheets for visible-light photocatalysis. Mater Today Commun 23:100903
Zhu M, Lu J, Hu Y, Liu Y, Hu S, Zhu C (2020) Photochemical reactions between 1, 4-benzoquinone and O_2·−. Environ Sci Pollut Res Int 27:31289–31299

Authors and Affiliations

A. N. Muhamad Hissam[1] · S. I. Sinar Mashuri[1,2] · N. F. Chayed[1,2] · N. H. Rozali Annuar[3] · N. Asikin-Mijan[4] · S. F. Ibrahim[5] · N. H. Othman[6] · G. AbdulKareem-Alsultan[7,8] · Y. H. Tan[9] · U. Rashid[10] · Y. H. Taufiq-Yap[7,8] · M. L. Ibrahim[1,2]

✉ M. L. Ibrahim
mohd_lokman@uitm.edu.my

[1] School of Chemistry and Environment, Faculty of Applied Sciences, Universiti Teknologi MARA, 40450 Shah Alam, Selangor, Malaysia

[2] Centre for Functional Materials and Nanotechnology, Institute of Science, Universiti Teknologi MARA, 40450 Shah Alam, Selangor, Malaysia

[3] Faculty of Applied Sciences, Universiti Teknologi MARA Cawangan Johor, Kampus Pasir Gudang, 81750 Masai, Johor, Malaysia

[4] Department of Chemical Sciences, Faculty of Science and Technology, Universiti Kebangsaan Malaysia, 43600 Bangi, Selangor Darul Ehsan, Malaysia

[5] Faculty of Applied Sciences, Universiti Teknologi MARA, Cawangan Pahang, Kampus Jengka, Universiti Teknologi MARA, 26400 Bandar Tun Abdul Razak Jengka, Pahang, Malaysia

[6] Hydrogen Program, R&D Department, Group Research & Technology (GR&T), Project Delivery & Technology (PD&T), PETRONAS Research Sdn Bhd, 43000 Kajang, Selangor Darul Ehsan, Malaysia

[7] Catalysis Science and Technology Research Centre (PutraCat), Faculty of Science, Universiti Putra Malaysia (UPM), 43400 Serdang, Selangor, Malaysia

[8] Department of Chemistry, Faculty of Science, Universiti Putra Malaysia (UPM), 43400 Serdang, Selangor, Malaysia

[9] Chemical and Energy Engineering, Faculty of Engineering, Universiti Teknologi Brunei, Gadong 1410, Brunei Darussalam

[10] Faculty of Applied Sciences, UCSI University, No 1, Jalan UCSI, UCSI Heights, Cheras, 56000 Kuala Lumpur, Selangor, Malaysia